

Thermal Analysis to Achieve Low Temperature with Thermoelectric Cooling System

Ali M. Ashour^{*}, Ali D. Salman^{**}, Ayad M. Salman^{***}

^{*}Mechanical Engineering Department, University of Technology, Baghdad, Iraq
Email: me.21.05@grad.uotechnology.edu.iq
<https://orcid.org/0009-0000-6684-6963>

^{**}Mechanical Engineering Department, University of Technology, Baghdad, Iraq
Email: Ali.d.salman@uotechnology.edu.iq
<https://orcid.org/0000-0003-2742-1852>

^{***}Mechanical Engineering Department, University of Technology, Baghdad, Iraq
Email: ayad.m.salman@uotechnology.edu.iq
<https://orcid.org/0000-0002-7334-554X>

Abstract

Thermoelectric coolers (TEC) are devices that conversion of electrical power into a temperature gradient. TEC modules have the benefits of high dependability, small dimensions, lightweight, absence of mechanical moving parts and working fluid. Thermoelectric cooling systems have experienced significant utilisation in recent years. These technologies have been used in automobiles to cool and maintain the quality of goods during transportation and in portable cooling bags, computers, and medical apparatus. The TEC manufacture datasheet only offers limited data on characteristics and maximum parameters, which is insufficient for studying thermoelectric systems. This paper presents an analytical modelling methodology that provides a direct method for assessing the performance of module parameters and determining the fundamental thermal physical parameters of a TEC. Furthermore, this article outlines the procedure for choosing the appropriate TEC module from a selection of three options to integrate it with a vapour compression refrigeration (VCR) system. The objective is to attain low temperatures while reducing power consumption and improving performance. The findings indicates that The TEC1-12706 module was the most suitable option among three different types of TEC modules for integration with the VCR system to achieve low temperatures. This choice was based on its lower power consumption than the TEC127010 and TEC127015 modules, resulting in 36.5% and 59.3% energy savings, respectively. Additionally, the heat dissipation from the hot side of the TEC12706 is lower than the TEC12710 and TEC12715 modules by 32.2% and 59%, respectively.

Keywords- Thermoelectric cooler; mathematical modelling; Seebeck effect; Peltier effect; thermoelectric cooling systems.

I. INTRODUCTION

Thermoelectric coolers modules enable converting electrical power into a temperature difference. This module employs the Peltier effect, which involves simultaneously heating and cooling the two opposing sides of the TEC module [1]. TEC modules have garnered growing attention due to their concurrent enhancement in economic and technical characteristics and their extensive range of applications. Consequently, the manufacturer of TEC has provided the market with a diverse range of modules that exhibit varying thermoelectric parameters, and shapes [2]. The selection of performance metrics for the TEC module, which include cooling capacity (Q_c), coefficient of performance (COP), and temperature difference (ΔT) between the cold and hot sides, are greatly affected by the specific practical application [3]. In the context of thermoelectric refrigerators utilized as air conditioning systems, the primary focus of optimization involves the performance indices of Q_c and COP, with respect to the given temperature difference. The TEC module is additionally employed to reduce the operational temperature of electronic devices. Therefore, the parameters ΔT and COP are commonly employed to assess the performance of TEC in electronic cooling applications, specifically in relation to the required cooling capacity [4]. Typically, the data sheets for a given TEC module display various characteristics and maximum allowed parameters. These parameters include the maximum temperature difference between the hot and cold sides of the TEC, the maximum current, the maximum supplying voltage, and the maximum absorbed heat from the cold side of the TEC [5]. The objective is to identify the TEC with the highest performance, enhance the operating parameters through basic calculations, and simulate the complete cooling system (comprising the TEC) using commercially accessible Computational Fluid Dynamics (CFD) software. To accomplish these tasks, it is imperative to know the fundamental physical properties of the TEC materials, namely electrical conductivity, Seebeck coefficient, and thermal conductivity, of the TEC materials. However, most manufacturers do not include such information within their product catalogues. As a result, the researchers often encounter challenges in acquiring these specific physical properties [6]. Huang et al. [7] experimented to accurately assess the physical properties of a TEC module. One issue is the limited accessibility of necessary equipment and

insufficient time for thermal designers to conduct the required measurements. In several studies, VCR and TEC have been combined to develop a hybrid refrigeration system. Fu et al.[8] investigated the use of a hybrid system (VCR-TEC) in small-capacity household refrigerators experimentally and theoretically. Their investigations revealed that by utilizing an additional 99.5 W of electricity to power the TEC system, they could obtain a temperature of $-38.1\text{ }^{\circ}\text{C}$ in the freezer chamber. Vián et al.[9] constructed a three-section hybrid household refrigerator that combines TEC and VCR. Their system includes a super-conservation section with TEC at $0\text{ }^{\circ}\text{C}$, a freezer at $-22\text{ }^{\circ}\text{C}$, and a refrigerator compartment with VCR at $4\text{ }^{\circ}\text{C}$. In addition, they created a computational model based on the finite differences method to develop and optimize this application. Their findings revealed that the hybrid refrigerator's total power consumption was around 48.1W. Astrain et al.[10] demonstrated the performance of a hybrid refrigerator with a freezer compartment, a cooler compartment, and a new chamber for a TEC at temperatures ranging from $(-4\text{ to }0)\text{ }^{\circ}\text{C}$. Their findings revealed that the configuration with the TEC modules located between the freezer and the TEC compartment consumes 10% less electricity than the configuration with the TEC modules set in the wall between the cooler and the TEC compartment, owing to the lower temperature of the TEC's hot side. Söylemez et al.[11-13] developed and evaluated a hybrid refrigerator that employs TEC and VCR. They observed that hybrid refrigerators use at least three times as much energy as standard refrigerators. The hybrid refrigerators moved 17.5 kg of load faster than the original refrigerators from an ambient temperature of $25\text{ }^{\circ}\text{C}$ to the target temperature of $2\text{ }^{\circ}\text{C}$. When they placed the TEC module in the middle of the side wall between the top and mid shelves, their projection findings based on a CFD model indicated uniform temperature distribution and air velocity inside the cabinet. Alghanima et al . [14] presented a numerical and experimental investigation that studied the effect of the cold-side heat sink's structure and fan's operating condition on the performance of a hybrid refrigerator's thermoelectric compartment at $2\text{ }^{\circ}\text{C}$. Their findings showed that increasing the fan speed from 500 to 2000 rpm improved the TEC's COP by roughly 20%. Furthermore, the temperature was uniformly raised by increasing the width and number of slots. Patil and Devade [15] Patil and Devade [24] studied air-cooled and water-cooled condensers in VCR and hybrid systems. According to their findings, the thermoelectric effect boosts the energy efficiency of a VCR by around 15.72% per year. As a result, the hybrid system's coefficient of performance is ultimately improved through improved temperature regulation during operation.

This paper illustrates a simple method for determining the physical properties of a TEC module using the data provided in the datasheet. The fundamental physical properties, namely the Seebeck coefficient, electrical resistivity, and thermal conductivity, can be calculated given the knowledge of the number of thermoelectric couples, the cross-sectional area, and the length of each thermoelectric element. Additionally, this article presents the method for selecting the suitable TEC module that integrates with a VCR system to achieve low temperatures with low power consumption and high performance. Combining TEC with VCR aims to achieve low temperatures at cold side of TEC, as shown in Figure (1). The combining of two systems happens by absorbing the heat released from the hot side of TEC by the evaporator of VCR system. So, the temperature of the cold side is extremely decreasing because of lower temperature at hot side of TEC.

II. MATHEMATICAL MODELING

The basic TEC circuit is shown in Figure (2). The heat is generated by Peltier cooling, half-joule heating, and thermal conduction [16, 17].

$$Q_C = Q_{Peltier} - \frac{1}{2}Q_{Joule} - Q_{conduction} \quad (1)$$

When the current is passed between two semiconductors, it is found that heat must be constantly added or removed at the junction to keep the temperature at the same value. This phenomenon is called the Peltier effect and is illustrated by the following:

$$Q_{Peltier} = \alpha T I \quad (2)$$

Where α is the Seebeck coefficient (volt/ $^{\circ}\text{C}$) as the following equation below, T is the temperature ($^{\circ}\text{C}$), and I is the electrical Current (A).

$$\alpha = \frac{V}{\Delta T} \quad (3)$$

Joule heating is the heat generated because of the electrical resistance of a current flow.

$$Q_{Joule} = I^2 R \quad (4)$$

Where R is the electrical resistance (Ω) as the following equation:

$$R = \frac{\gamma L}{A} \quad (5)$$

Where γ : is the electrical resistivity ($\Omega \text{ m}$), L is the length of a thermoelement (m), and A is the cross-sectional area of a thermoelement (m^2).

The thermal conduction heat as the following equation:

$$Q_{conduction} = k A \frac{\Delta T}{L} \quad (6)$$

Where k is the thermal conductivity ($\text{W/m } ^\circ\text{C}$)

The amount of heat rejected from the hot side is [18]:

$$Q_h = \alpha T_h I + \frac{1}{2} I^2 R - k A \frac{\Delta T}{L} \quad (7)$$

Where T_c , T_h is the cold and hot side temperatures ($^\circ\text{C}$), respectively, and ΔT is the temperature difference between the hot and cold sides ($^\circ\text{C}$).

According to the first law of thermodynamics across the thermoelectric cooler, the input power will be:

$$P_{TEC} = Q_h - Q_c \quad (8)$$

Substitute Equations (6) and (7) in (8), the input power will be:

$$P_{TEC} = \alpha I (T_h - T_c) + I^2 R \quad (9)$$

To determine the COP for the TEC system, where it represents the ratio between heat absorbed by the cold side to the power consumed, as shown below.

$$COP_{TEC} = \frac{Q_c}{P_{TEC}} \quad (10)$$

I_{max} , V_{max} , ΔT_{max} , and T_h are parameters that the majority of Peltier manufacturers have set. So, by employing the technical data of the TEC module, the mathematical modeling parameters are [19, 20]:

$$\alpha = \frac{V_{max}}{T_h} \quad (11)$$

$$R = \frac{(T_h - \Delta T_{max}) V_{max}}{T_h I_{max}} \quad (12)$$

$$K = \frac{(T_h - \Delta T_{max}) V_{max} I_{max}}{2 T_h \Delta T_{max}} \quad (13)$$

$$V = \alpha \Delta T + I R \quad (14)$$

Where K is the thermal conductance ($\text{W}/^\circ\text{C}$) as follows:

$$K = \frac{kA}{L} \quad (15)$$

Figure (3) shows a flow chart employed to determine the thermoelectric parameters using EES software.

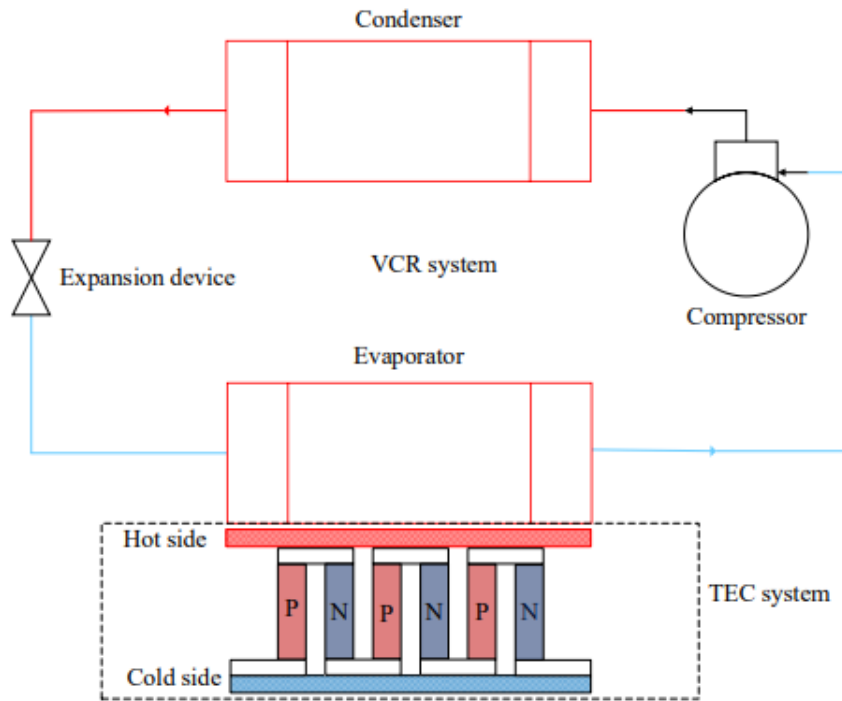


Fig. 1 schematic diagram of TEC-VCR system.

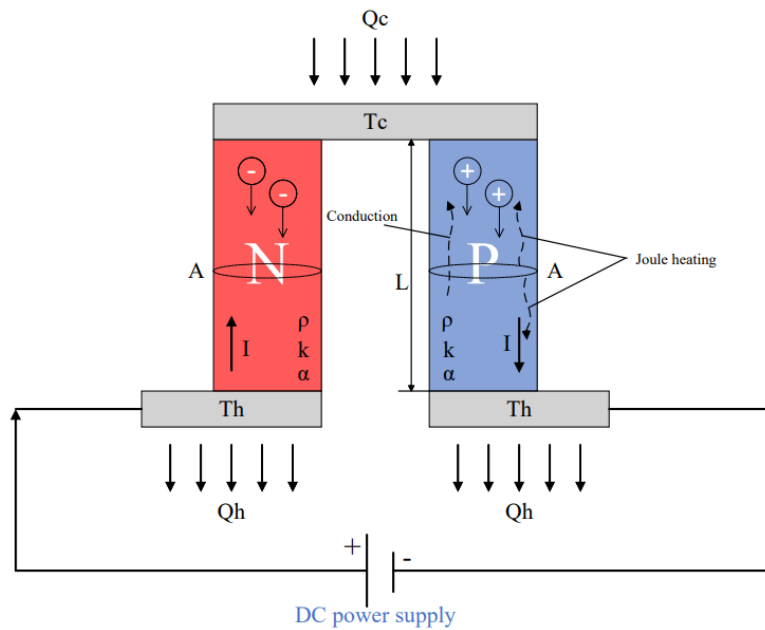


Fig. 2 Basic electrical circuit component for TEC.

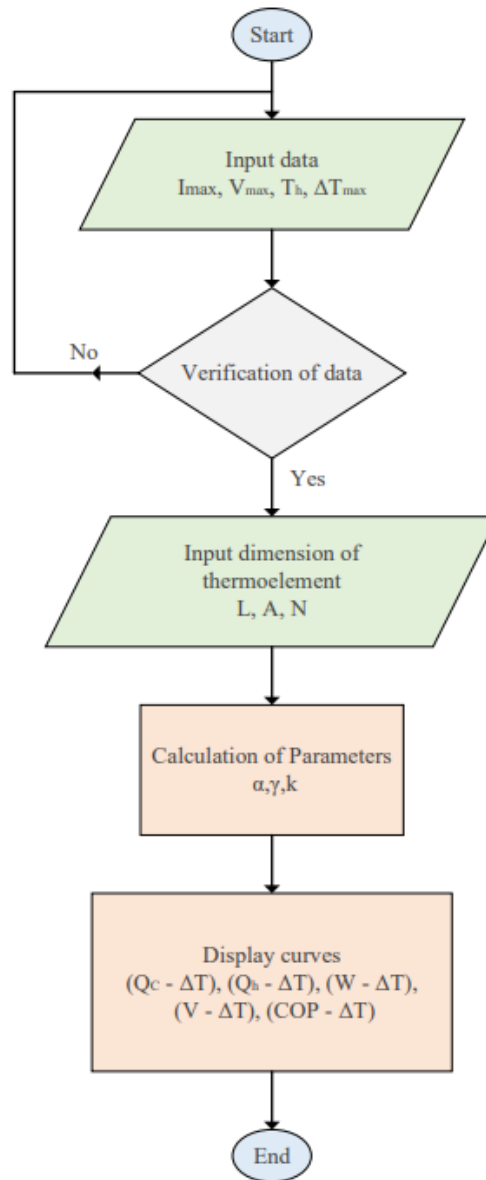


Fig. 3 Flow chart to determine Parameters of TEC.

III. NUMERICAL MODELING FOR TEC MODULE

the geometric structure of the TEC is shown in Figure (4). The basic unit of the TEC consists of the n-type and p-type thermoelements. Modeling at element assumes that both types of thermoelements are similar except for the Seebeck effect's opposite direction. The TEC geometric construction comprised 127 pairs of thermoelement sized $1.2 \times 1.2 \times 1.2 \text{ mm}^3$. With overall dimensions of $40 \times 40 \times 3.8 \text{ mm}^3$, the thermoelements TEC are assembled electrically in series and thermally in parallel. Each pair of P/N-type thermoelements are connected in series by $1.2 \times 3.6 \times 0.3 \text{ mm}^3$ copper electrodes. The copper electrodes of the hot and cold sides are uniformly arrayed on a $40 \times 40 \text{ mm}^2$ ceramic plate. 1 mm thick Alumina (Al_2O_3) ceramic plates have adhered to both sides of the TEC. The mesh of the geometry has 38022 elements, as shown in Figure (5). The properties of the P/N-type thermoelements were calculated from the programming performance of the TEC using the EES program, as presented in the previous section. The properties of the material are listed in Table (1).

Table (1): Properties of the materials of TEC.

Material	α (volt/ $^\circ\text{C}$)	k (W/m K)	γ ($\Omega \text{ m}$)
P-type	2.1×10^{-4}	2.9	5.7×10^{-6}
N-type	2.1×10^{-4}	2.9	5.7×10^{-6}

Copper	-	401	1.69×10^{-8}
Ceramic	-	4.5	-

In this study, the temperature of the hot side of the TEC is assumed equal to the temperature of the evaporator for the VCR to achieve low temperature, and the voltage supply to the TEC is also known according to typical operating conditions. Therefore, the hot side temperature and the input voltage are two boundary conditions. Table (2) details the boundary conditions for typical operating conditions.

Table (2): Boundary conditions of the TEC.

V_{in} (volt)		5.5	6.5
V_{out} (volt)		0	
T_h (°C)	Case 1	-14	
	Case 2	-18	

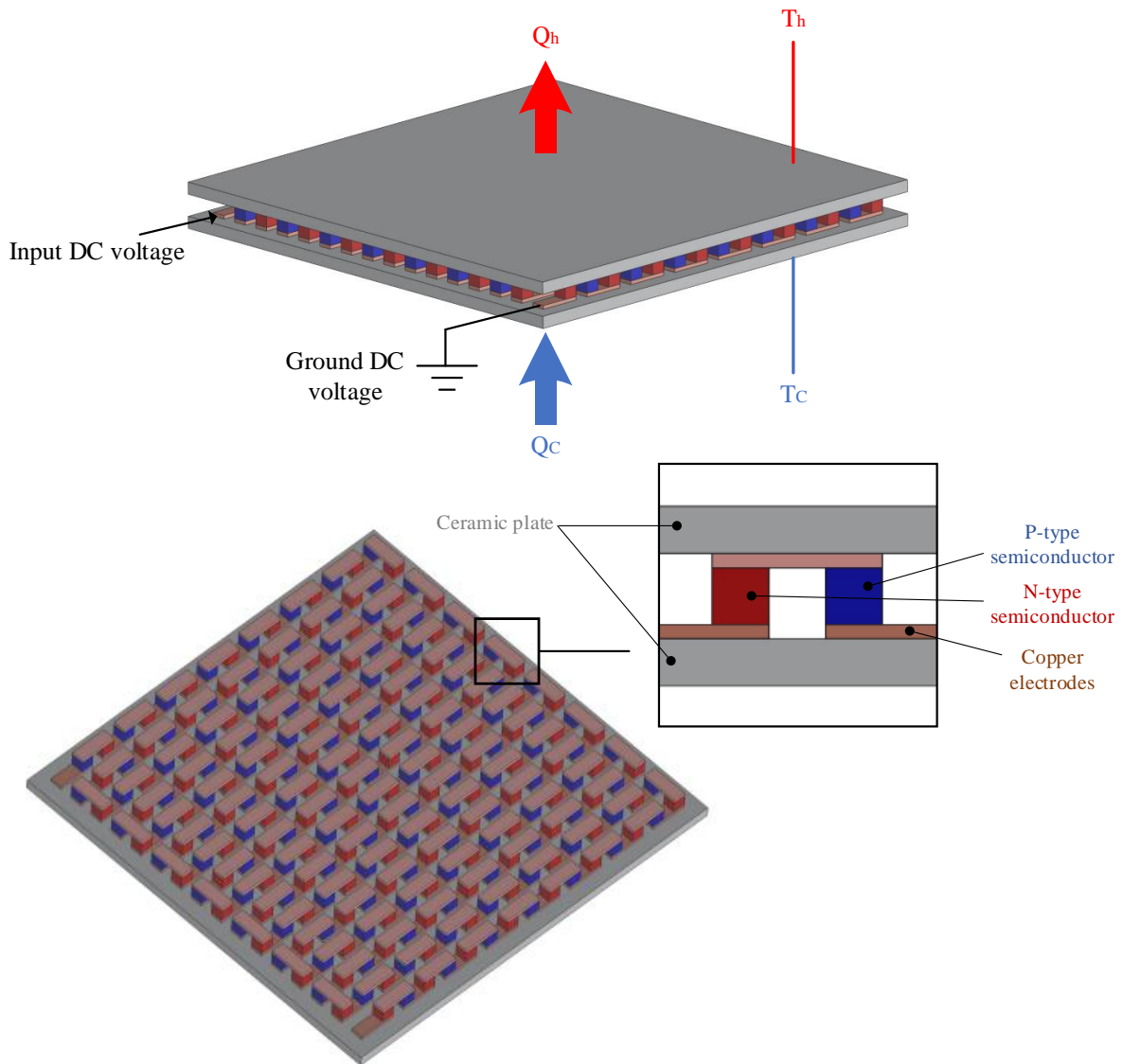


Fig. 4 The structure of TEC1-12706.

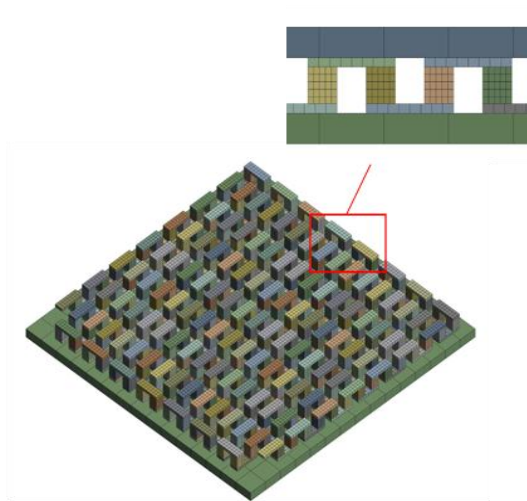


Fig. 5 Mesh generated of TEC.

In order to predict and estimate the performance of TEC and optimize their design, a computational model with multiple physical field couplings containing the current continuity equation, the energy conservation equation, and the thermoelectric coupling equation under stationary conditions is developed [21-23].

$$\nabla \cdot \vec{J} = 0 \quad (16)$$

$$\nabla \cdot \vec{q} = \dot{q} \quad (17)$$

$$\vec{J} = -[\sigma] \nabla \varphi - [\sigma][\alpha] \nabla T \quad (18)$$

$$\vec{q} = [\alpha] T \vec{J} - [k] \nabla T \quad (19)$$

From the above equations, the governing equation coupling electric potential and temperature can be obtained as the following equation:

$$\nabla([\sigma] \nabla \varphi - [\sigma][\alpha] \nabla T) = 0 \quad (20)$$

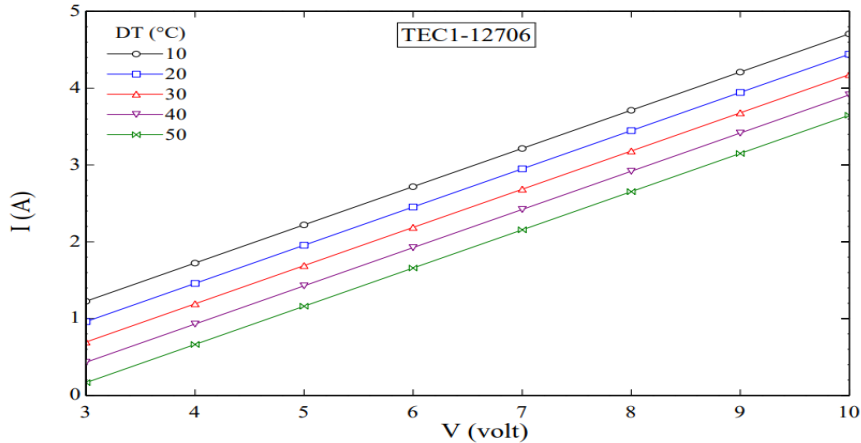
$$\frac{\vec{J}}{\sigma} - T \vec{J} (\nabla \alpha)_T - T \vec{J} \left(\frac{\partial \alpha}{\partial T} \right) \nabla T + \nabla([k] \nabla T) = 0 \quad (21)$$

where \vec{J} represents the current density, \vec{q} the heat flux, and \dot{q} the heat generation. $[\sigma]$ is the matrix of the coefficient of electrical conductivity, $[k]$ is the matrix of the coefficient of thermal conductivity, and φ is the scalar of the electrical potential [24]. On the left-hand side of Equation (21) are the Joule heat, Peltier heat, Thomson heat, and conduction. After determining the current, Equations (20) and (21) can be solved to determine the distribution of potential and temperature and then obtain other parameters. However, the thermoelectric parameters vary with temperature, resulting in nonlinear equation-solved values. Therefore, the equations are solved using a finite element simulation.

IV. RESULTS AND DISCUSSION

The selection of the suitable TEC module depends on many parameters, such as the voltage applied, the limitation of hot and cold side temperatures, and the difference between them with their derivatives' relation. The consumed DC current depends on other parameters, where the main goal is to arrive at the design condition for the hybrid system with a suitable TEC module. The TEC module's selection depends on comparing the theoretical results for three TEC modules TEC1-127...06,10,15. All the comparison results depend on a main assumption that the temperature of the cold side is equal to constant ($T_c = -45^\circ\text{C}$). Figure (6) depicts the characteristic curves for the relationships between each DC voltage applied and current consumed with the selective differences in temperature ($T_h - T_c$) between the hot and cold side temperatures. According to the results of the theoretical relationship so, Figure (7) depicts the relation between the power consumed with different voltage values applied at variance ($T_h - T_c$) and can see that power consumed is directly proportional to the voltage applied and inversely to the temperature difference, highest power consumption by TEC1-127.15,10 then 06. Other results are shown in Figure (8), where cooling capacity is directly proportional to the voltage applied and inversely to temperature difference. This figure shows the highest cooling capacity that can get from TEC1-12715. The same behavior for heat released from the hot side can be shown in Figure (9). One of the most important to select a TEC module is the COP. Figure (10) shows the relationship between COP and other traditional parameters, such as voltage applied and temperature difference, also other hidden parameters that can affect the COP value, like the thermal conductive value between the hot and cold side of the TEC module. So, by comparing the performance parameters for three TEC modules based on the theoretical analysis above, the results show that TEC1-12706 is suitable depending on the cooling capacity and power consumed beside the COP, as shown in Figure (11), with lower power consumed and heat release. The results of the current study differ numerically from those of Ziyad et al. [23] in work for a personal cooler, but the trend of the curves, as indicated in Figure (12), is the same.

The results of the temperature gradient of TEC are under various conditions of operating depending on the input voltage and the hot side temperature. Figure (13) presents the temperature gradient between the hot and cold sides of the TEC. The results show a decrease in the temperature of the cold side with increasing the voltage applied. However, this decrease in the cold side temperature is accompanied by a rise in the temperature of the hot side. When operating TEC at 5.5 volts and subjected to -14°C on the hot side, the results show that the maximum temperature on the hot side equals -11.17°C , and the minimum temperature on the cold side is -46.6°C . While operating TEC with 6.5 volts, the difference between the subjected and maximum temperatures increased due to increased heat release from the hot side of TEC., where the maximum temperature is -9.98°C and subjected to -14°C at the hot side. In contrast, the minimum temperature is -50.06°C on the cold side. If the subjected temperature on the hot side decreased, the cold side temperature reduced by 6.86 % at 6.5 volts and 8.32 % at 5.5 volts for TEC.



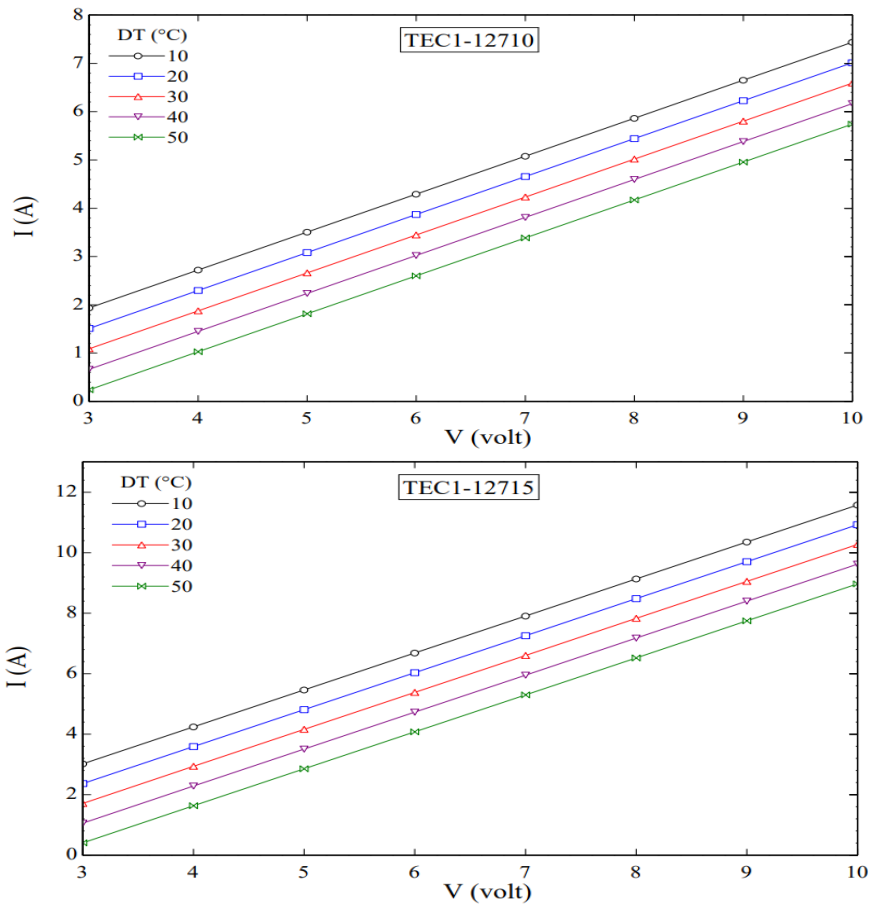
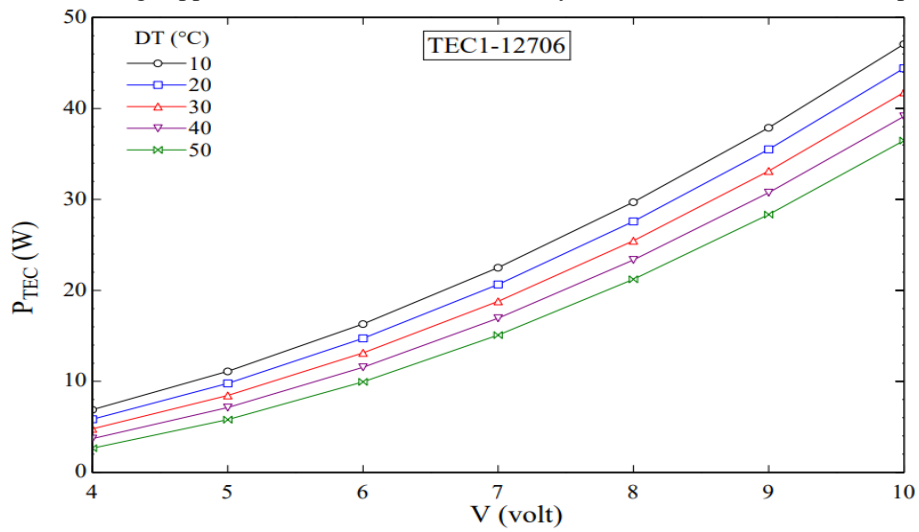


Fig. 6 Relationship between DC voltage applied of TEC with current for many TEC modules at selective temperature differences.



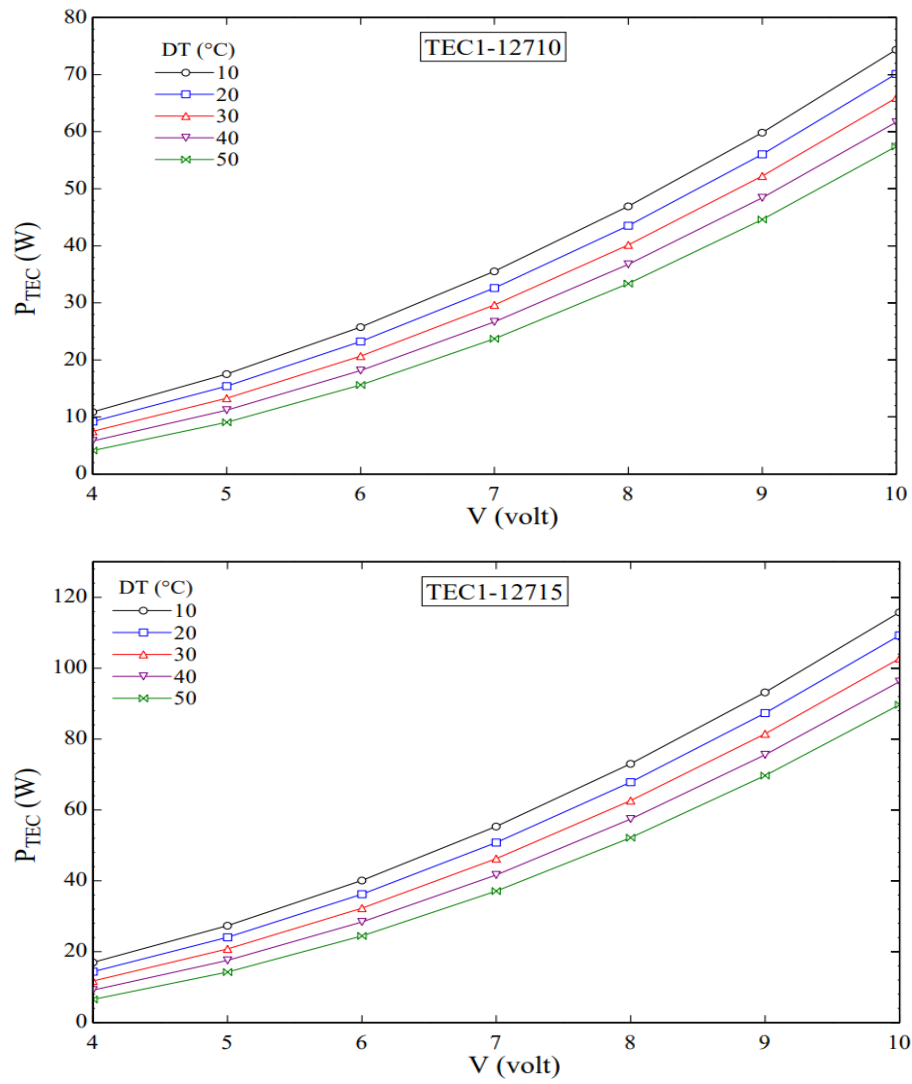
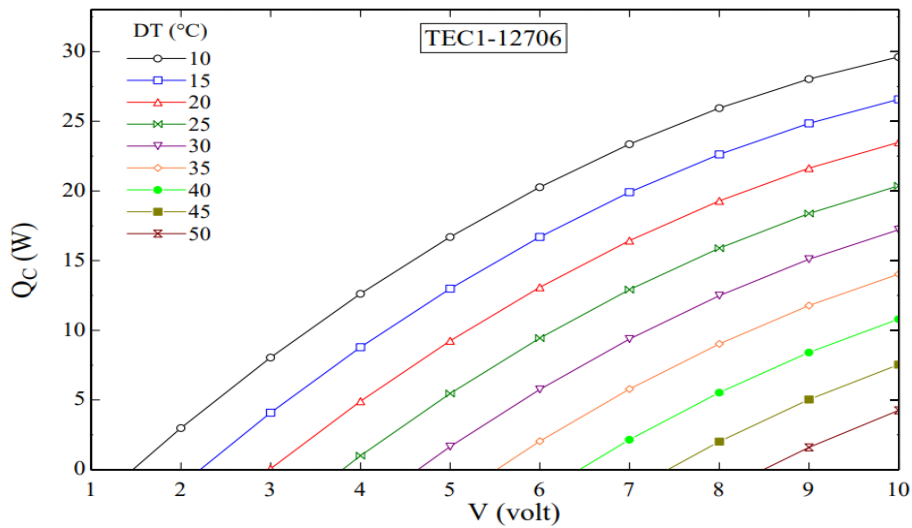


Fig. 7 Relationship between DC power consumed with voltage applied at variance difference in temperature for three types of TEC modules.



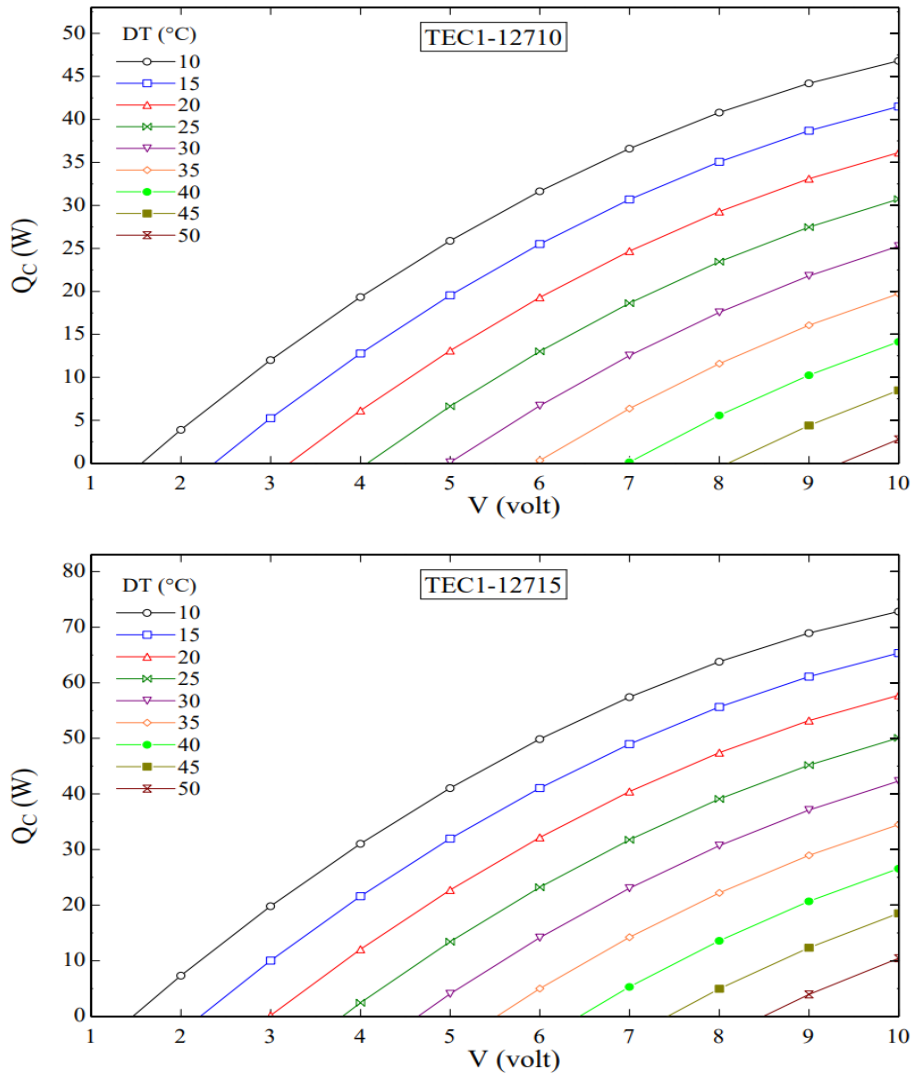
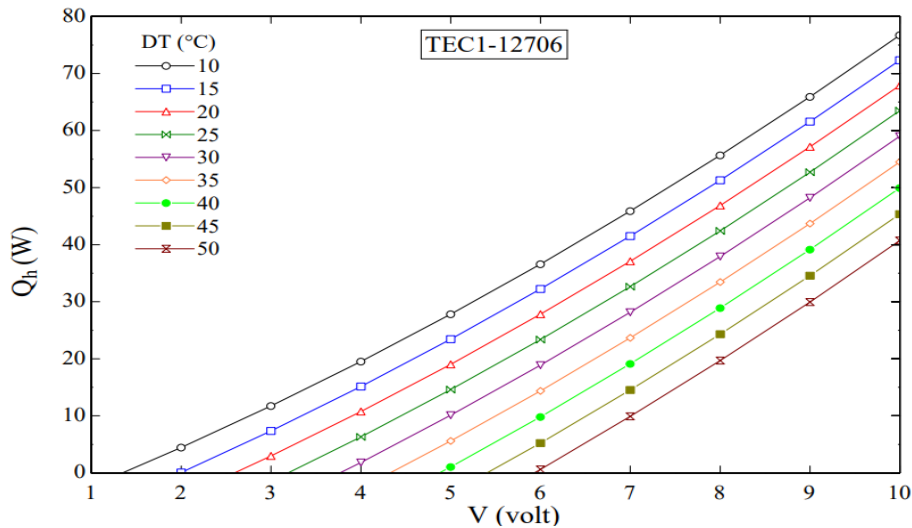


Fig. 8 Relationship between cooling capacity with voltage applied and temperature difference for three types of TEC modules.



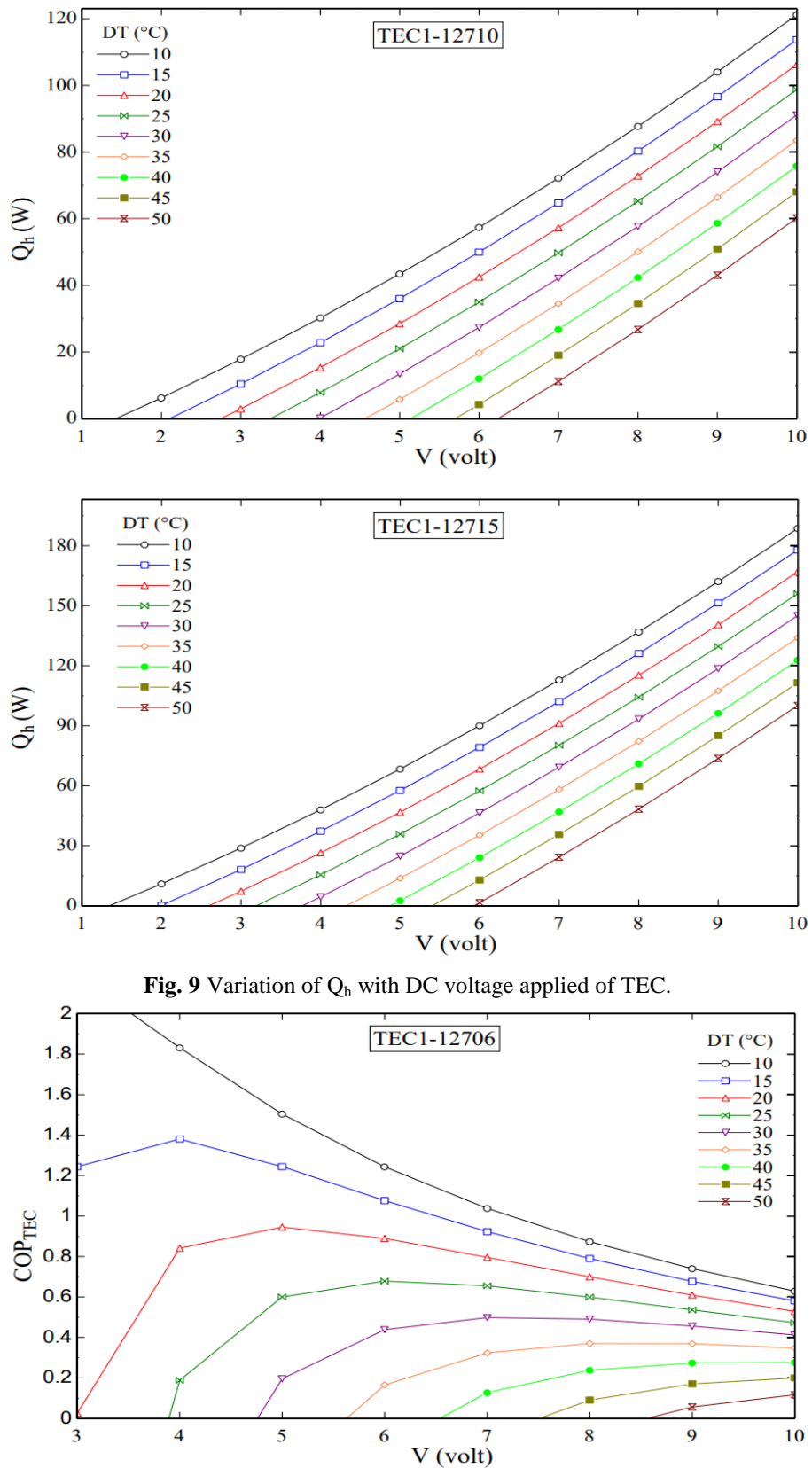


Fig. 9 Variation of Q_h with DC voltage applied of TEC.

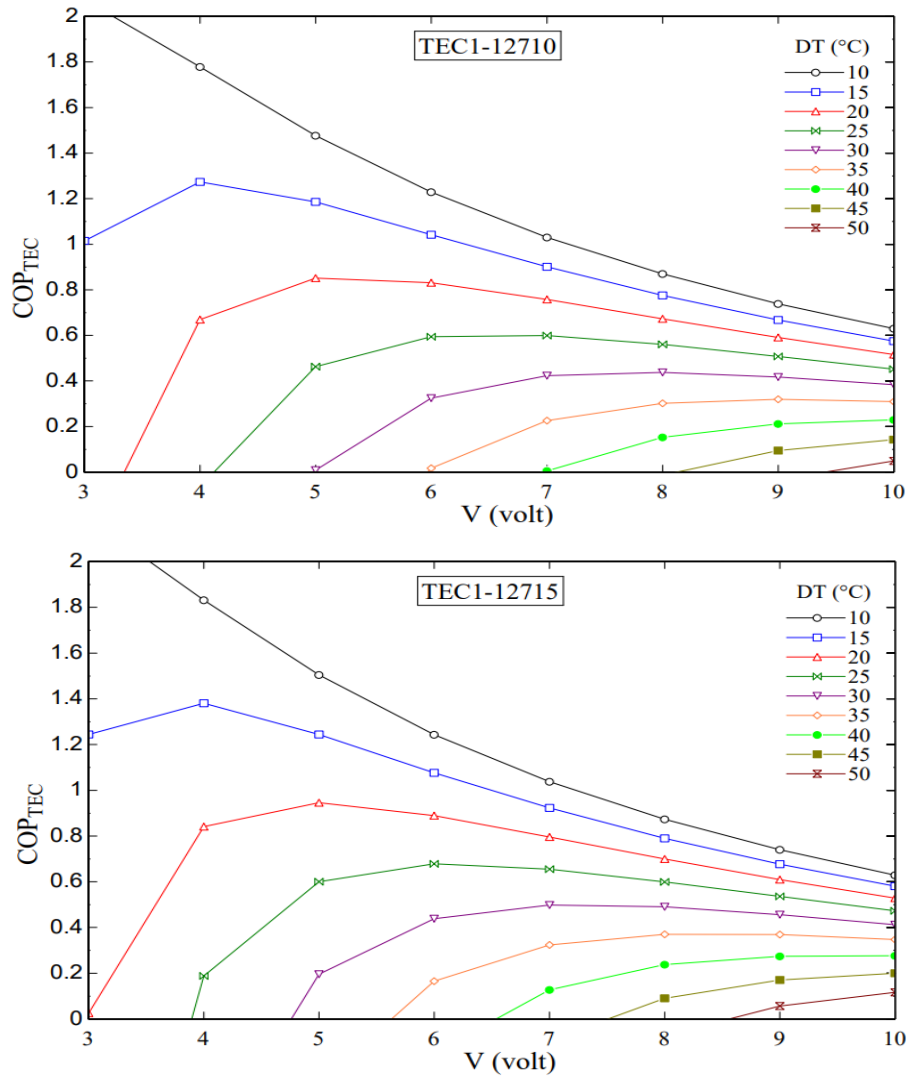


Fig. 10 COP with different values for voltage applied and temperature difference.

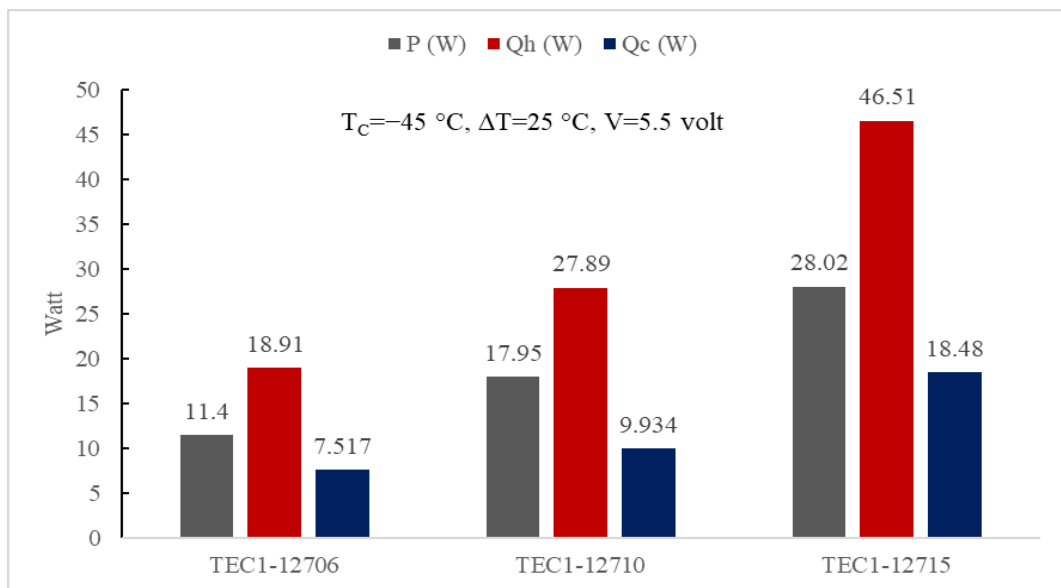
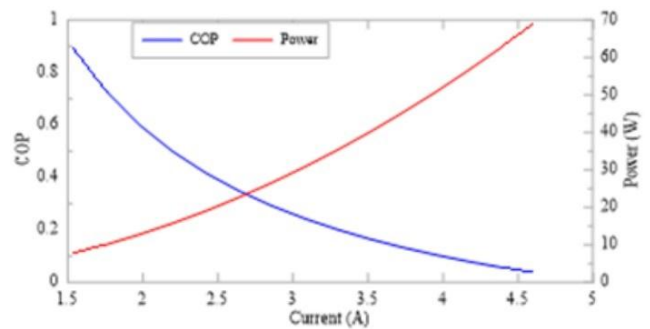
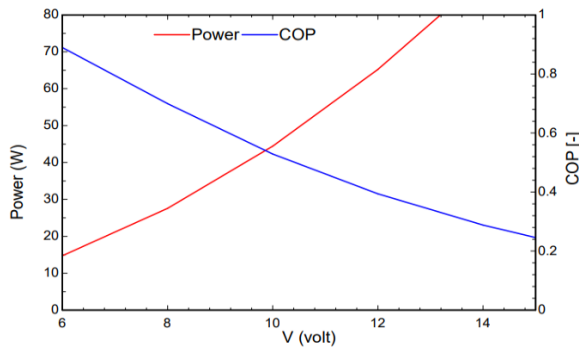
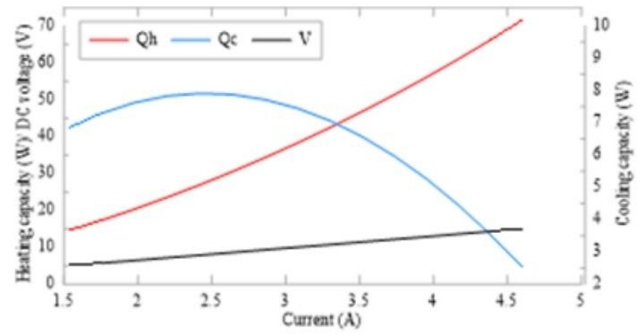
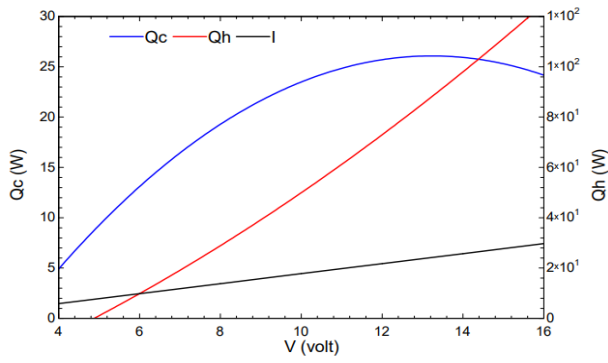


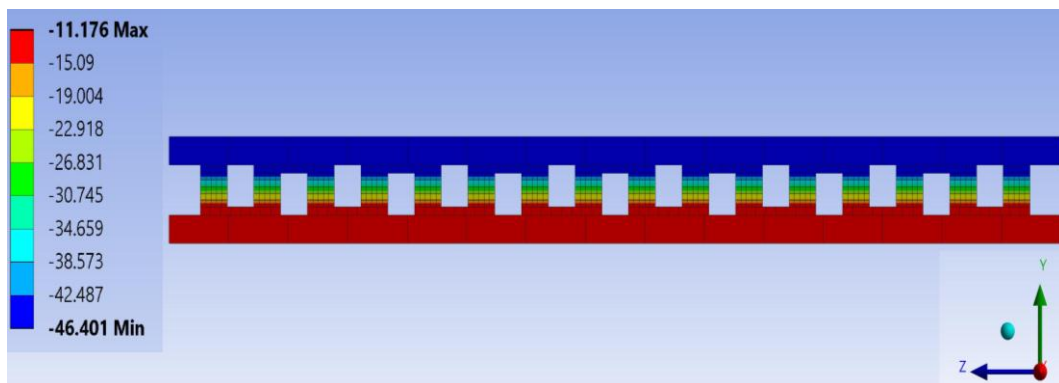
Fig. 11 Comparison of results for TEC module at same working condition.



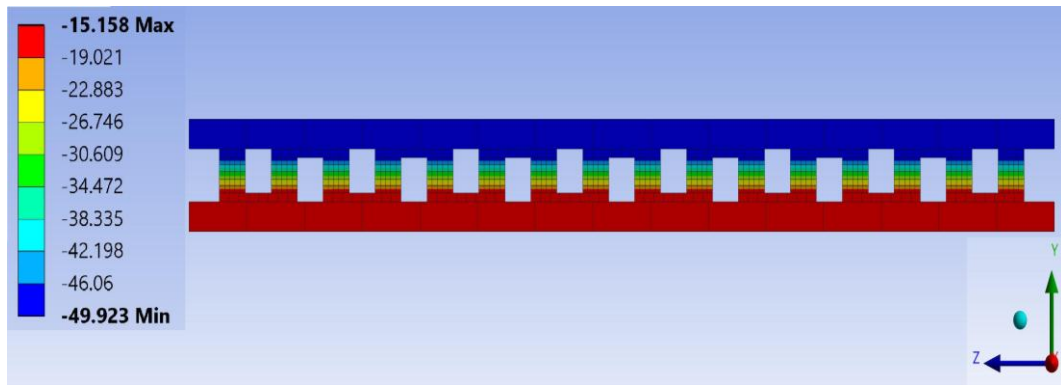
a) current study

b) Work of Ziyad et al.[20]

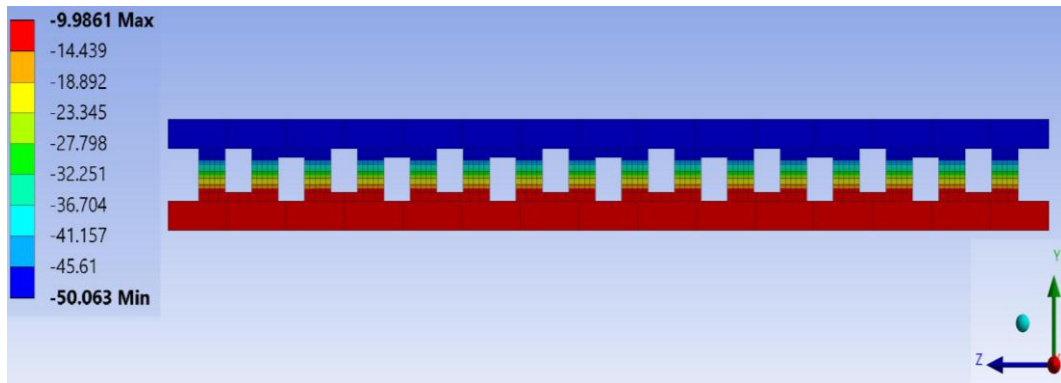
Fig. 12 comparison between current study and previous studies.



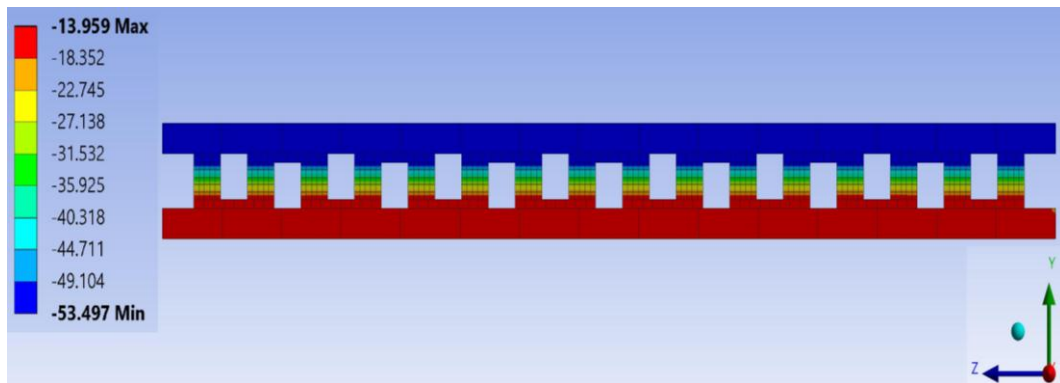
a) 5.5 volts of the TEC, and $T_h = -14\text{ }^\circ\text{C}$



b) 5.5 volts of the TEC, and $T_h = -18\text{ }^\circ\text{C}$



c) 6.5 volts of the TEC, and $T_h = -14\text{ }^\circ\text{C}$



d) 6.5 volts of the TEC, and $T_h = -18\text{ }^\circ\text{C}$

Fig. 13 The temperature gradient in the TEC.

V. CONCLUSION

The following conclusions can be drawn based on this study

<http://doi.org/10.58564/IJSER.2.3.2023.87>

<https://ijser.aliraqia.edu.iq>

- The paper introduces an analytical modelling approach that offers a straightforward means of evaluating the performance of module parameters and determining TEC's fundamental thermal physical parameters.
- Increasing the voltage increases the current at each temperature difference. Also, increasing power consumption is due to increasing the current.
- The heat absorbed from the cold side of TEC (Q_c) decreases at a certain voltage with increasing the temperature difference.
- Decreasing the Q_c caused at the same voltage applied decreases the heat release (Q_h) from the hot side of TEC based on the first law of thermodynamics. Therefore, Q_h decreases with increasing temperature difference at a certain voltage.
- TEC1-12706 was the optimal choice of three types of TEC modules to integrate with VCR system to attain low temperature due to lower power consumption and heat release from the hot side.

REFERENCES

- [1] H. Lee, *Thermal design: heat sinks, thermoelectrics, heat pipes, compact heat exchangers, and solar cells*: John Wiley & Sons, 2022.
- [2] S. B. Riffat and X. Ma, "Thermoelectrics: a review of present and potential applications," *Applied thermal engineering*, vol. 23, pp. 913-935, 2003.
- [3] T. Yin and Z.-Z. He, "Analytical model-based optimization of the thermoelectric cooler with temperature-dependent materials under different operating conditions," *Applied Energy*, vol. 299, p. 117340, 2021.
- [4] S. M. Pourkiaei, M. H. Ahmadi, M. Sadeghzadeh, S. Moosavi, F. Pourfayaz, L. Chen, *et al.*, "Thermoelectric cooler and thermoelectric generator devices: A review of present and potential applications, modeling and materials," *Energy*, vol. 186, p. 115849, 2019.
- [5] tetch. *Peltier - Thermoelectric Cooler Modules*. Available: www.tetch.com
- [6] Z. Luo, "A simple method to estimate the physical characteristics of a thermoelectric cooler from vendor datasheets," *Electronics cooling*, vol. 14, pp. 22-27, 2008.
- [7] B.-J. Huang, C. Chin, and C. Duang, "A design method of thermoelectric cooler," *International journal of Refrigeration*, vol. 23, pp. 208-218, 2000.
- [8] Z. G. Q. R.P. Fu, W.Q. Tao , X.B. Zhu, J.R. Liu "Experimental and numerical study on performance of hybrid refrigeration system that combines vapor compression and thermoelectric systems," *Applied Thermal Engineering*, vol. 194, 2021.
- [9] D. A. J.G. Vián "Development of a hybrid refrigerator combining thermoelectric and vapor compression technologies," *Applied Thermal Engineering*, vol. 29, 2009.
- [10] A. M. D. Astrain*, A. Rodríguez, "Improvement of a thermoelectric and vapour compression hybrid refrigerator," vol. 39, 2012.
- [11] E. A. Engin Söylemez , Ayhan Onat "Experimental analysis of hybrid household refrigerators including thermoelectric and vapour compression cooling systems," vol. 95, pp. 93-107, 2018.
- [12] E. A. Engin Söylemez , Ayhan Onat , Yalçın Yükselentürk , Selim Hartomacıo ğlu, "Numerical (CFD) and experimental analysis of hybrid household refrigerator including thermoelectric and vapour compression cooling systems," *International Journal of Refrigeration*, vol. 99, pp. 300-315, 2019.
- [13] E. A. Engin Söylemez , Ayhan Onat , Selim, "CFD analysis for predicting cooling time of a domestic refrigerator with thermoelectric cooling system," vol. 123, pp. 138-149, 2021.
- [14] Yasser Abdulrazak Alghanima , Osama Mesalhy , Ahmed Farouk AbdelGawad, "Effect of cold-side heat sink configurations on thermal performance of thermo-electric compartment of a hybrid household refrigerator," *Case Studies in Thermal Engineering*, vol. 37, 2022.
- [15] K. D. D. Sagar D. Patil, "Increasing Energy Efficiency of Domestic Refrigerator Using Single Thermoelectric Module & Water Cooling of Condenser," *International Journal of Latest Trends in Engineering and Technology (IJLTET)*, vol. 5, 2015.
- [16] D. Zhao, Tan, Gang, "A review of thermoelectric cooling: materials, modeling and applications," *Applied thermal engineering*, vol. 66, pp. 15-24, 2014.
- [17] D. A. J.G. Vián "Development of a thermoelectric refrigerator with two-phase thermosyphons and capillary lift," *Applied Thermal Engineering*, vol. 29, pp. 1935-1940, 2009.
- [18] M. Siahmargoi, N. Rahbar, H. Kargarsharifabad, S. E. Sadati, and A. Asadi, "An experimental study on the performance evaluation and thermodynamic modeling of a thermoelectric cooler combined with two heatsinks," *Scientific Reports*, vol. 9, p. 20336, 2019.
- [19] K. Khamil, M. Sabri, A. Yusop, R. Mohamed, and M. Sharuddin, "Modelling and simulation of the performance analysis for Peltier module and Seebeck module using MATLAB/simulink," *Jurnal Kejuruteraan*, vol. 32, pp. 231-238, 2020.

- [20] Z. Tark, A. J. Hamed, and A. H. N. Khalifa, "Performance Study of the Thermoelectric Personal Cooler under Different Ambient Temperatures," *International Journal of Heat & Technology*, vol. 40, 2022.
- [21] J. Zhang, X. Song, X. Zhang, Q. Zhang, and H. Zhao, "Performance analysis and optimization of the rough-contact Bi₂Te₃-based thermoelectric cooler via metallized layers," *Case Studies in Thermal Engineering*, vol. 40, p. 102522, 2022.
- [22] E. E. Antonova and D. C. Looman, "Finite elements for thermoelectric device analysis in ANSYS," in *ICT 2005. 24th International Conference on Thermoelectrics, 2005.*, 2005, pp. 215-218.
- [23] H. Liu, X. Zhao, G. Li, and X. Ma, "Investigation of a novel separately-configured micro-thermoelectric cooler to enabling extend application scope," *Applied Energy*, vol. 306, p. 117941, 2022.
- [24] G. Fraisse, J. Ramousse, D. Sgorlon, and C. Goupil, "Comparison of different modeling approaches for thermoelectric elements," *Energy conversion and management*, vol. 65, pp. 351-356, 2013.